

Collisional and Radiative Energy Loss of Heavy Quarks

J. Aichelin¹, **P.B. Gossiaux**, **T. Gousset**

SUBATECH, Laboratoire de Physique Subatomique et des Technologies Associées,
Université de Nantes - IN2P3/CNRS - Ecole des Mines de Nantes
4 rue Alfred Kastler, F-44072 Nantes, Cedex 03, France

E-mail: aichelin@subatech.in2p3.fr

Abstract. Heavy quarks are one of the key tools to study the properties of the expanding plasma created in ultrarelativistic heavy ion collisions. In this context we develop a framework to study the $Qq \rightarrow Qgg$ collisions in scalar QCD and provide the results for different key quantities. We investigate the radiative energy loss and compare the results to the collisional energy loss. We conclude that radiative and collisional energy loss together allow for a description of the recently published ALICE data.

1. Introduction

The study of the properties of a plasma of quarks and gluons (QGP) which existed some milliseconds after the Big Bang and which can very probably be produced in the collisions of ultrarelativistic heavy ions is the main objective of the presently ongoing experiments at RHIC (Brookhaven/United States) and CERN (Switzerland & France) in which a couple of thousand physicists are involved. The challenge is to find this state of matter and to identify its properties although its lifetime is extremely short (10-23 s) and the spatial extension is of the order of 10-14 m. Then a transition from partons to the hadrons occurs and only the hadrons can be finally observed in the detectors. At the phase transition the measured multiplicity of light hadrons is well described by statistical models, but presently it is not obvious if this statistical equilibrium is achieved already when the QGP is created or only shortly before the hadronization takes place or even by means of the hadronization process itself. The answer to this question is essential for understanding the plasma properties.

Quantum Chromo Dynamics (QCD), the underlying theory of the strong interaction, predicts that two and three particle correlations, the precursors of hadrons, are already formed above the critical temperature T_c in the QGP phase and the few calculations of the viscosity in a QGP indicate that only close to the phase transition the viscosity is sufficiently small to bring or maintain the expanding QGP to local equilibrium. On the other hand ideal hydrodynamical models which are based on the assumption that the local equilibrium is established already at the beginning of the QGP expansion and that the phase transition is sudden at a critical energy density (Cooper Frye assumption), can predict many observables. Presently it is not clear whether this is a true verification of the assumption of a local equilibrium during the expansion

¹ invited speaker



or whether the rather unknown initial conditions of the plasma expansion is at the origin of this agreement. The fact that the centrality dependence of several observables cannot be described and, even in central collisions, a couple of observables cannot be correctly predicted, may also be considered as a hint for non-equilibrium effects.

In order to assess directly the properties of the plasma during the expansion of the plasma it is necessary to concentrate on those probes which do not come to an equilibrium with the plasma. Heavy quarks and jets are such probes. Especially heavy quarks (charm and beauty) are well suited for that - due to their large mass they are produced dominantly by hard processes during the early stage of the reaction when the QGP is formed. Their initial creation in a hard process is predicted to be very similar as in proton-proton collisions and is therefore directly accessible by experiment. While traversing the plasma the heavy quarks do not come to equilibrium with the environment since their interaction with the partons of the plasma is not strong enough. However, due to the exchange of the momentum in the partonic interactions, the final momentum distribution of heavy quarks (and, as a consequence of the observed heavy mesons) contains information on the number of scattering partners as well as on the momentum transfer during the QGP phase. Both depend on whether the dynamical evolution of the expanding system occurs in equilibrium or not. The heavy mesons are therefore a decisive tool to study the nature of the expansion and the properties of the plasma.

Heavy quarks are produced in hard binary initial collisions between the incoming protons. Their production cross sections are known from pp collisions and can as well be calculated in pQCD calculations. Therefore the initial transverse momentum distribution of the heavy quarks is known. Comparing this distribution with that measured in heavy ion collisions allow to define $R_{AA} = (d\sigma_{AA}/dp_t^2) / (N_c d\sigma_{pp}/dp_t^2)$, where N_c is the number of the initial binary collisions between projectile and target. The deviation of R_{AA} from one measures the interaction of the heavy quark with the plasma because the hadron cross sections of heavy mesons are small. The heavy quark does not come to thermal equilibrium with the QGP therefore R_{AA} contains the information on the interaction of the heavy quark while it traverses the plasma.

Unfortunately the experimental results depend not only on the elementary interaction but also on the description of the expansion of the QGP [1]. Therefore the ultimate aim is to control the expansion by results on the light meson sector. This has not been achieved yet for the LHC and therefore it is difficult to assess the influence of the expansion on the observables. We use here the approach from Kolb and Heinz which has reasonably well described the midrapidity light mesons at RHIC [2]. We adjust only the charged particle multiplicity to the value measured at LHC.

The R_{AA} of 0.2 values observed for large p_t heavy mesons are much smaller than originally expected. Early theoretical approaches based on perturbative QCD (pQCD) calculation gave much larger values and it has been doubted, whether pQCD is the right tool to describe this interaction. This early calculation, however, used ad hoc assumptions on the coupling constant α_s and the infrared regulator μ . With a standard choice μ and α_s an artificial K factor, an overall multiplication factor of the elastic cross section of around 10 [3, 4] had to be introduced to match the experimental data.

A while ago we advanced an approach for the collisional energy loss of heavy quarks in the QGP [5, 6, 7]. Our matrix element has the same form as pQCD calculations in first order Born approximation with a infrared regulator μ . The infrared regulator is, however, not taken as constant but proportional to the Debye mass with a constant of proportionality which is chosen in that way that we obtain the same energy loss as calculations which employ a hard thermal loop for scattering with a low momentum transfer. In addition we employ a coupling constant determined by the sum rule advanced by Dokshitzer and later used by Peshier. Both these improvements increase the cross section especially for small momentum transfers and reduced therefore the necessary K factor to 2. For details we refer to [5, 6, 7]

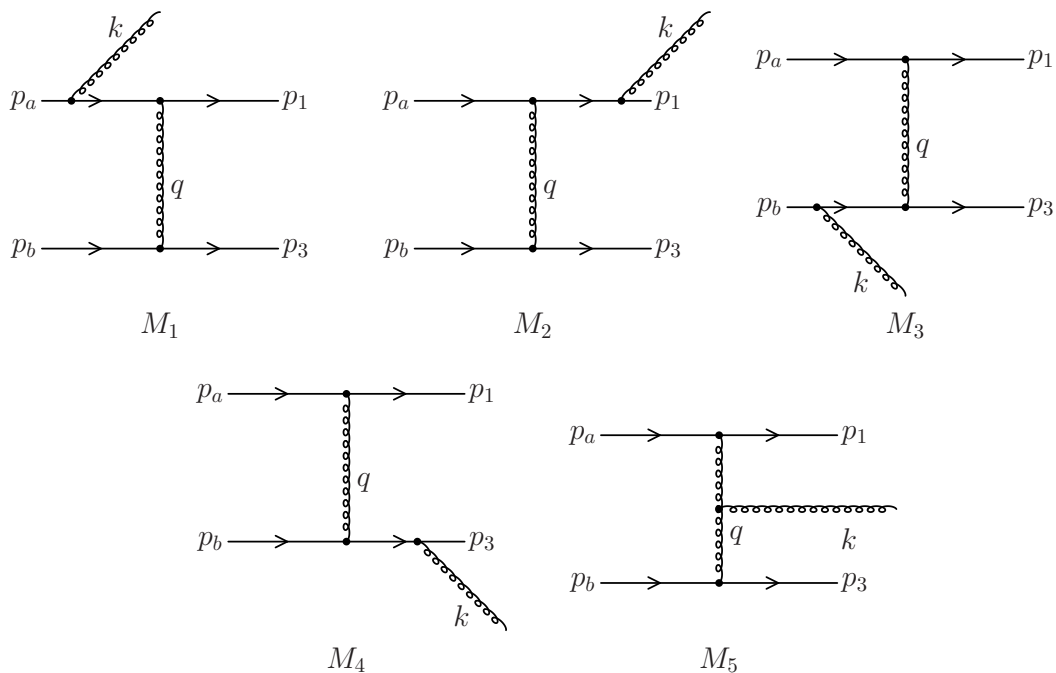


Figure 1. (Color online) The five matrix elements which contribute to the gluon bremsstrahlung.

In addition to the energy loss by elastic collisions the particle loose energy as well by radiation. The is the dominant form of energy loss for light mass quarks but plays as well an important role for heavy quarks. It is the purpose of these proceedings to study these inelastic collisions in detail and to investigate their influence for the energy loss in heavy ion collisions [8, 9].

2. Radiative Energy Loss

Extending our collisional energy loss approach to radiative energy loss we have to consider the following 5 processes whose matrix elements are displayed in fig.1. The commutation relation

$$T^b T^a = T^a T^b - i f_{abc} T^c \quad (1)$$

allows us to regroup the 5 matrix elements into 3 combinations, each of them being independently gauge invariant:

$$\begin{aligned} iM_{h.q.}^{QED} &= C_a i(M_1 + M_2) \\ iM_{l.q.}^{QED} &= C'_a i(M_3 + M_4) \\ iM^{QCD} &= C_c i(M_1 + M_3 + M_5). \end{aligned} \quad (2)$$

h.q. (l.q.) mark the emission of the gluon from the heavy (light quark) line. C_a , C'_a and C_c are the color algebra matrix elements. The matrix elements labeled as QED are the bremsstrahlung diagrams already observed in Quantum Electrodynamics (QED), whereas that labeled QCD is the genuine diagram of Quantum Chromodynamics (QCD). The QCD diagram is the main objet of interest here because it dominates the energy loss of heavy quarks.

We evaluate the matrix elements in scalar QCD (see ref.[13]). They are given by

$$iM_1^{SQCD} = C_A (ig)^3 \frac{(p_b + p_3)^\mu}{(p_3 - p_b)^2} D_{\mu\nu} [p_3 - p_b] \left(\frac{(p_a + p_1 - k)^\nu (2p_a - k)^\epsilon}{(p_a - k)^2 - m^2} - \epsilon^\nu \right)$$

$$\begin{aligned}
iM_5^{SQCD} &= C_c (ig)^3 D^{\mu\mu'} [p_3 - p_b] D^{\nu\nu'} [p_1 - p_a] [g_{\mu'\nu'} (p_a - p_1 + p_3 - p_b)_\sigma + \\
&\quad g_{\nu'\sigma} (p_1 - p_a - k)_{\mu'} + g_{\sigma\mu'} (p_b - p_3 + k)_{\nu'}] \epsilon^\sigma \\
&\quad \cdot \frac{(p_3 + p_b)^\mu (p_a + p_1)^\nu}{(p_3 - p_b)^2 (p_1 - p_a)^2}
\end{aligned} \tag{3}$$

M_3 is obtained by replacing $p_a \rightarrow p_b$ and $p_1 \rightarrow p_3$ in M_1 . To discuss the physics we adopt the following light cone vectors

$$\begin{aligned}
p_a &= \left\{ \sqrt{s - m^2}, \frac{m^2}{\sqrt{s - m^2}}, 0, 0 \right\} \\
p_b &= \{0, \sqrt{s - m^2}, 0, 0\} \\
k &= \{x\sqrt{s - m^2}, 0, \vec{k}_t\} \\
p_1 &= p_a + q - k = \left\{ p_a^+ (1 - x) - \frac{q_t^2}{p_b^-}, \frac{(\vec{k}_t - \vec{q}_t)^2 + m^2}{(1 - x)p_a^+}, \vec{q}_t - \vec{k}_t \right\} \\
p_3 &= p_b - q = \left\{ \frac{q_t^2}{p_b^-}, p_b^- - \frac{(1 - x)k_t^2 - x(\vec{k}_t - \vec{q}_t)^2 + m^2 x^2}{p_a^+ (1 - x)x}, -\vec{q}_t \right\}
\end{aligned} \tag{4}$$

Here we study only the dominant QCD terms.

Using light cone gauge and integrating over seven phase space variables the cross section can be written as [9]

$$\frac{d\sigma^{Qq \rightarrow Qgq}}{dx d^2 k_t d^2 q_t} = \frac{1}{2(s - m^2)} |M|^2 \frac{1}{4(2\pi)^5 \sqrt{\Delta}} \Theta(\Delta). \tag{5}$$

The calculation of this cross section is straight forward but not transparent. $|M|^2$ diverges for small momentum transfer q_t^2 . Therefore we have to introduce a multiplicative infrared regulator

$$G(q_t^2, \mu) = \frac{q_t^4}{(q_t^2 + \mu^2)^2}. \tag{6}$$

The regulated cross section

$$\frac{d\bar{\sigma}^{Qq \rightarrow Qgq}}{dx d^2 k_t d^2 q_t} = G(q_t^2, \mu) \cdot \frac{d\sigma^{Qq \rightarrow Qgq}}{dx d^2 k_t d^2 q_t} \tag{7}$$

can only be solved numerically and we employ a Monte Carlo procedure. This solution we call model I. In the limit

$$s, xs \gg |q_t^2|, \vec{k}_t^2 \tag{8}$$

$|M|^2$ simplifies and we obtain [9]

$$|M|^2 = 16\pi^3 x(1 - x) |M_{el}|^2 \cdot P_g(m, \vec{q}_t, \vec{k}_t, x) \tag{9}$$

with the regularized elastic matrix element

$$|M_{el}|^2 = \frac{2}{9} \frac{g^2 4s^2}{(q_t^2 + \mu^2)^2} \tag{10}$$

and

$$P_g(m, \vec{q}_t, \vec{k}_t, x) = \frac{C_A \alpha_S (1 - x)}{x\pi^2} \left(\frac{\vec{k}_t}{\vec{k}_t^2 + x^2 m^2} - \frac{\vec{k}_t - \vec{q}_t}{(\vec{k}_t - \vec{q}_t)^2 + x^2 m^2} \right)^2 \tag{11}$$

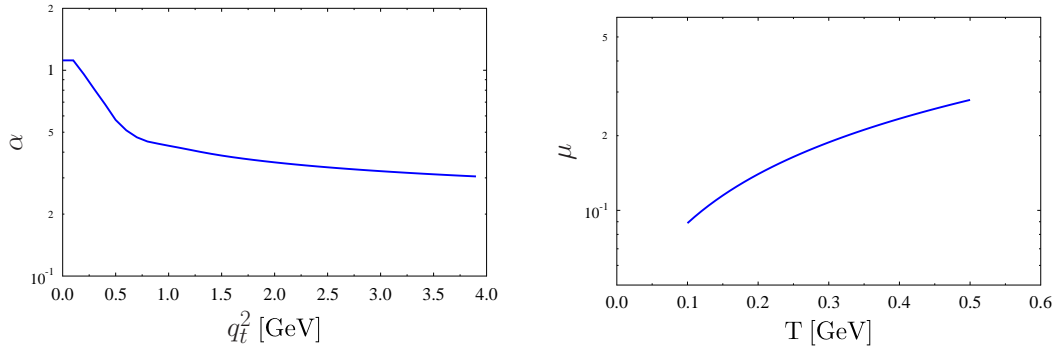


Figure 2. (Color online) Left: the running coupling constant as a function of the momentum transfer q_t^2 . Right: The infrared regulator $\mu(T)$ as a function of the temperature.

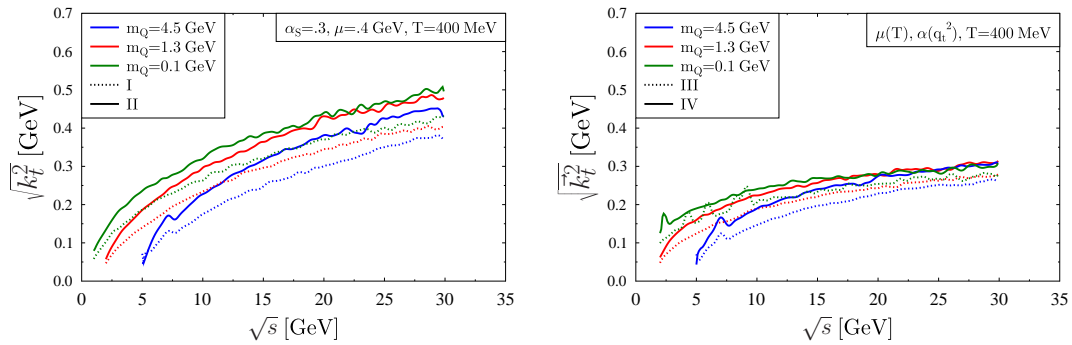


Figure 3. (Color online) Average transverse momentum of the emitted gluon, $\sqrt{\langle k_t^2 \rangle}$, as a function of \sqrt{s} for different masses of the heavy quark. On the left hand side we display the results of the models I and II, on the right hand that of the models III and IV.

is the distribution function of the produced gluons. In the limit of vanishing heavy quark masses this model corresponds to the Gunion Bertsch approach ref. [10]. This model we call model II.

For the expanding plasma we go one step further and adopt the results of refs. [5, 6, 7] by introducing in eq. 6 a running coupling constant at the vertices of the exchanged gluon and a temperature depending infrared regulator. Both are displayed in fig. 2. For the gluon emission we keep a constant coupling constant $\alpha_S = 0.3$. These features are introduced by multiplying the square of the matrix elements of the models I and II by

$$\frac{a_S^2(q_t^2)(q_t^2 + \mu^2)^2}{\alpha_S^2 \cdot (q_t^2 + \mu(T)^2)^2}. \quad (12)$$

The modified full solution we call model III and the high energy approximation model IV. These 4 models we use now to study some key quantities which characterize the reaction. Fig.3 displays the average transverse momentum $\sqrt{\langle k_t^2 \rangle}$ of the emitted gluon as a function of \sqrt{s} . The left hand side shows this observable for the models I and II, the right hand side that for the models III and IV. We display the results for three different heavy quark masses, $m = .1, 1.3$ and 4.5 GeV. We see an increase of $\sqrt{\langle k_t^2 \rangle}$ with increasing \sqrt{s} because more energetic collisions

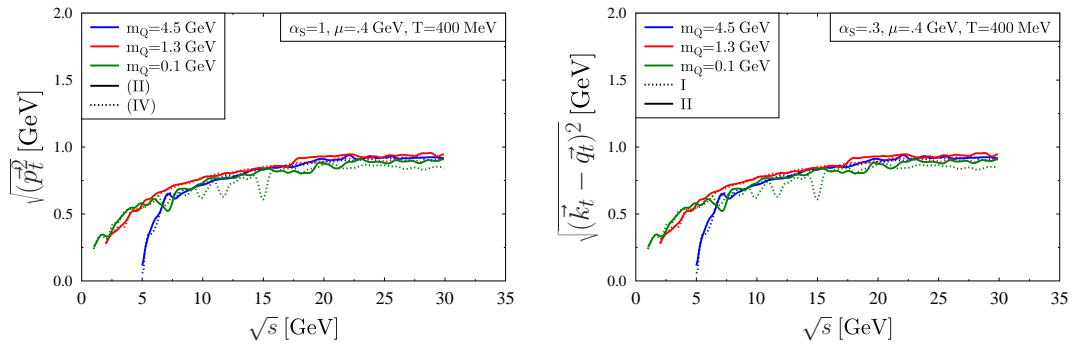


Figure 4. (Color online) Average transverse momentum transfer to the heavy quark $\sqrt{\langle \vec{p}_t^2 \rangle} = \sqrt{\langle (\vec{k}_t - \vec{q}_t)^2 \rangle}$ as a function of \sqrt{s} for different masses of the heavy quark. On the left hand side we display the results of the models I and II, on the right hand that of the models III and IV.

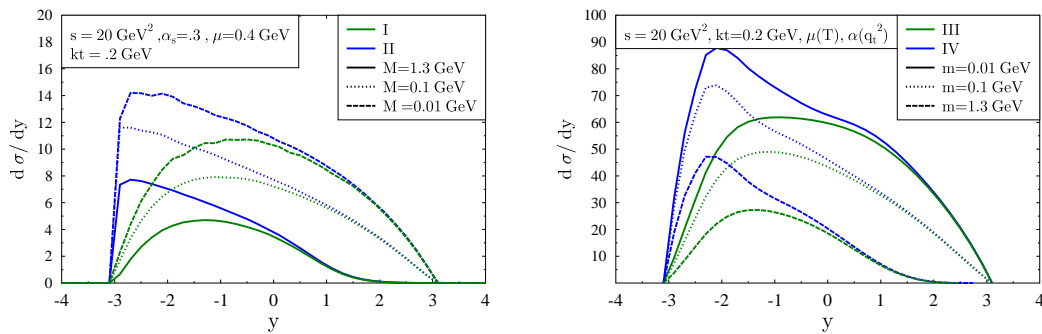


Figure 5. (Color online) Rapidity dependence of the cross section for different masses of the heavy quark. On the left hand side we display the results for the models I and II, on the right hand that for the models III and IV.

yield a larger momentum transfer between projectile and target quark. Clearly the running coupling constant favors low momentum transfers, q_t^2 , which yields consequently lower values of $\sqrt{\langle k_t^2 \rangle}$. Also the increase of $\sqrt{\langle k_t^2 \rangle}$ with \sqrt{s} is more moderate. The full solution yields smaller $\sqrt{\langle k_t^2 \rangle}$ values than the high energy approximation. It is remarkable that despite of the dead cone effect [11] the $\sqrt{\langle k_t^2 \rangle}$ of heavy quarks is smaller than that of light quarks.

Another quantity of interest is the final transverse momentum given to the heavy quark. This quantity is displayed in fig. 4 for different masses of the heavy quark. The left hand side shows this observable for the models I and II, the right hand side for the models III and IV. $\sqrt{\langle (\vec{k}_t - \vec{q}_t)^2 \rangle}$ is almost independent of the heavy quark mass and the high energy approximation reproduces the full solution very well. As already observed for $\sqrt{\langle k_t^2 \rangle}$ we find as well for $\sqrt{\langle (\vec{k}_t - \vec{q}_t)^2 \rangle}$ that a running coupling constant suppresses a large momentum transfer and hence the final transverse momenta of the outgoing particles is smaller. This is

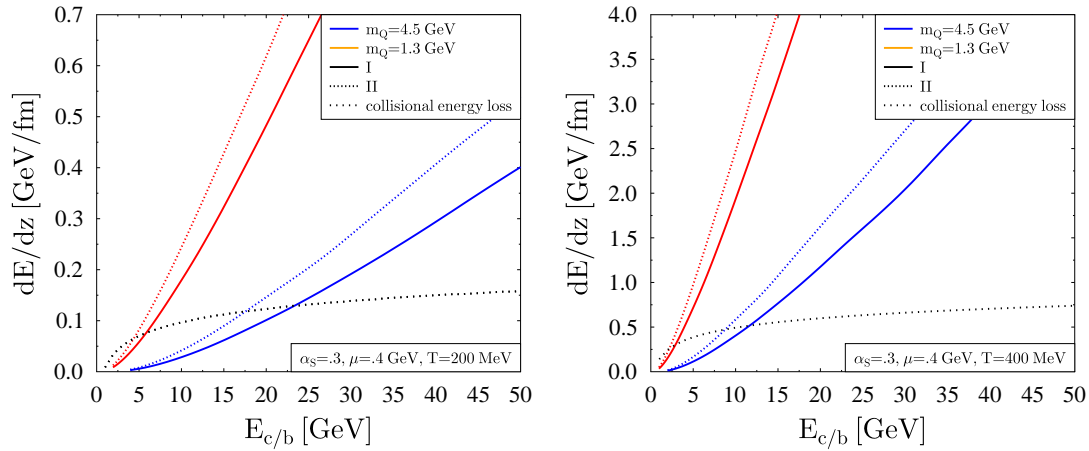


Figure 6. (Color online) Radiative and collisional energy loss as a function of the energy of the heavy quark for the models I and II, left for a temperature of $T=200$ MeV, right for $T=400$ MeV.

clearly seen by comparing the upper and the lower red lines of the right figure which compare directly $\sqrt{\langle (\vec{k}_t - \vec{q}_t)^2 \rangle}$ of the 4 models. In contradistinction to $\sqrt{\langle k_t^2 \rangle}$, $\sqrt{\langle (\vec{k}_t - \vec{q}_t)^2 \rangle}$ is -besides threshold effects - for a running coupling constant (almost) independent of \sqrt{s} and also independent of the mass of the heavy quark.

The rapidity dependence of the cross section

$$\frac{d\sigma^{Qq \rightarrow Qgq}}{dy d^2 k_t d^2 q_t} \propto x \frac{d\sigma^{Qq \rightarrow Qgq}}{dx d^2 k_t d^2 q_t} \quad (13)$$

is shown in fig. 5, on the left hand side for the models I and II, on the right hand side for the models III and IV. We see how the finite heavy masses shift the center of the distribution from $y = 0$ zu negative y values. We observe as well that the high energy approximation is valid for positive y values only whereas for negative y values, corresponding to $x < \frac{\sqrt{k_t^2}}{\sqrt{s}}$, the conditions for the approximations are not anymore satisfied and strong deviations appear. The running coupling constant and the introduction of $\mu(T)$ increase the cross section by a factor up to seven, especially for small x values.

The collisional and radiative energy loss due to the scattering of the heavy quark with light quarks are compared in fig.6 for the models I and II. The collisional energy loss in the scattering of a heavy quark with a light quark of the plasma is calculated as [12]

$$\frac{dE}{dz} = \frac{4\pi}{3} a_s^2 T^2 \frac{n_f}{6} \log\left(\frac{ET}{\mu^2}\right) \quad (14)$$

with a coupling constant of $\alpha_s = .3$, an infrared cut off of $\mu=.4$ GeV and a temperature of $T=200$ MeV (left) and 400 MeV (right). E is the incident energy of the heavy quark and the number of flavours, n_f , is taken as three. The radiative energy loss is obtained by the approximate formula

$$\frac{dE}{dz} = \int \int \frac{d^3 k}{(2\pi)^3} \rho(k) E x \frac{d\sigma_{rad}}{dx}(\sqrt{s}) dx \quad (15)$$

assuming that $\sqrt{s} = \sqrt{m^2 + 6ET}$. We see that for low energies of the heavy quark the collisional energy loss is larger than the radiative energy loss but already for moderate energies the radiative

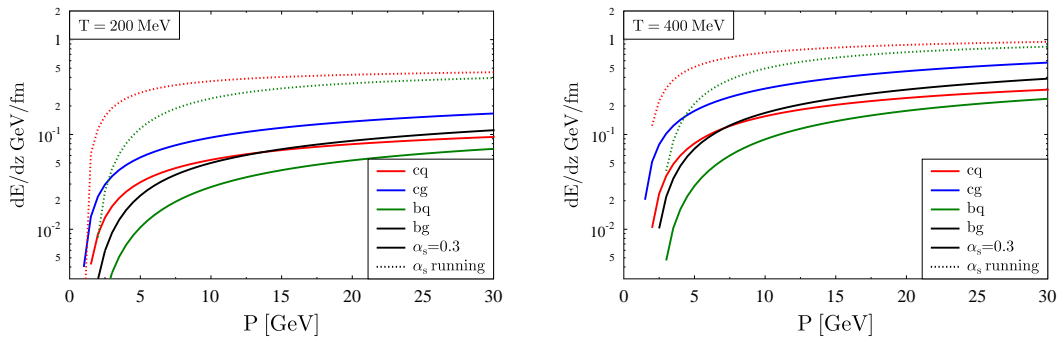


Figure 7. (Color online) The collisional energy loss for fixed α_S and μ as compared to running α_S and $\mu(T)$ for the temperatures $T=200\text{MeV}$ (left) and $T=400\text{ MeV}$ (right).

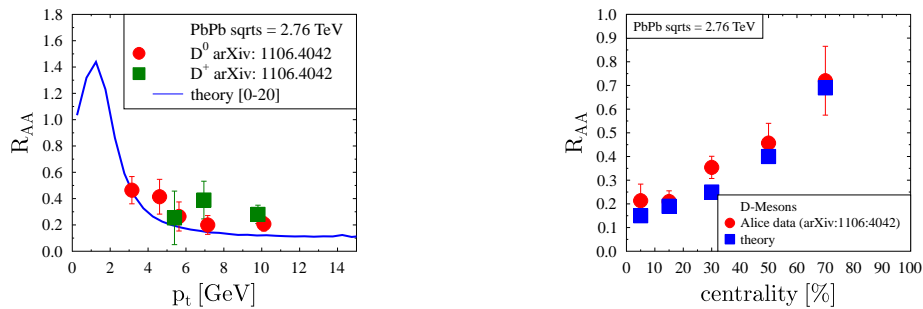


Figure 8. (Color online) Left: The calculated $R_{AA}(p_t)$ spectrum in comparison with the experimental data. Right: The p_t integrated $R_{AA}(p_t)$ spectrum for different centralities.

energy loss dominates. Finally we compare in fig.7 the collisional energy loss for fixed α_S and μ with running α_S and $\mu(T)$ for the temperatures $T=200\text{MeV}$ (left) and $T=400\text{ MeV}$ (right). cq, cg, bq and bg refer to charm-light quark, charm-gluon, bottom-light quark and bottom-gluon collisions, respectively. As for the radiative cross section we see also for the elastic cross section a strong enhancement and consequently a larger energy loss when α_S is running and μ becomes a function of the temperature $\mu(T)$.

If we include now both, the radiative energy loss and the collisional energy loss, calculated with running coupling constant and temperature dependent $\mu(T)$, in our calculation of the heavy quark energy loss in an expanding plasma in which the plasma is modeled by the hydrodynamical calculations of Kolb and Heinz [2] we describe [14] the recently measured $R_{AA}(p_t)$ values (the p_t spectrum measured in heavy ion collisions divided by that in pp collisions properly normalized by the total number of elementary collisions in heavy ion reactions) of the Alice collaboration almost quantitatively. This is shown in fig. 8, where on the left hand side $R_{AA}(p_t)$ is compared to the Alice data, whereas on the right hand side the centrality dependence of the p_t integrated spectrum is displayed.

In conclusion, we have studied how radiative collisions between a heavy and a light quark change the momentum of the heavy quark. We have shown the rapidity spectra of the emitted gluons and their average transverse momentum as well as the average transverse momentum transfer to the heavy quark. In these studies the full SQMD matrix element has been employed and compared to an approximate high energy formula which reduces to the Gunion Bertsch approach for vanishing heavy quark masses. We have demonstrated how an effective coupling constant and a temperature dependent infrared regulator, which we have developed in the framework of elastic collisions between heavy and light quarks, can be introduced in the radiation cross section and have studied how this changes the cross section. Finally we have shown that with these ingredients the measured R_{AA} values can be reproduced when the model is employed in an expanding plasma scenario.

- [1] P. B. Gossiaux, S. Vogel, H. van Hees, J. Aichelin, R. Rapp, M. He and M. Bluhm, arXiv:1102.1114 [hep-ph].
- [2] P. F. Kolb and U. W. Heinz, arXiv:nucl-th/0305084. published in *Quark Gluon Plasma*, World Scientific
- [3] G. D. Moore and D. Teaney, Phys. Rev. C **71** 064904 (2005).
- [4] B. Svetitsky, Phys. Rev. D **37** (1988) 2484.
- [5] P. B. Gossiaux, J. Aichelin Phys. Rev. **C78**, 014904 (2008), arXiv:0802.2525 [hep-ph]
- [6] P. B. Gossiaux, R. Bierkandt and J. Aichelin arXiv:0901.0946 [hep-ph]
- [7] P. B. Gossiaux and J. Aichelin arXiv:0901.2462 [nucl-th]
- [8] P. B. Gossiaux, J. Aichelin, T. Gousset and V. Guiho, J. Phys. G **37**, 094019 (2010) [arXiv:1001.4166 [hep-ph]].
- [9] J. Aichelin, P.B. Gossiaux and T. Gousset, to be published
- [10] J. F. Gunion and G. Bertsch, Phys. Rev. D **25** (1982) 746.
- [11] Y. L. Dokshitzer and D. E. Kharzeev, Phys. Lett. B **519** (2001) 199 [arXiv:hep-ph/0106202].
- [12] S. Peigne and A. V. Smilga, Phys. Usp. **52** (2009) 659 [Usp. Fiz. Nauk **179** (2009) 697] [arXiv:0810.5702 [hep-ph]].
- [13] E. Meggiolaro, Phys. Rev. D **53** (1996) 3835 [arXiv:hep-th/9506043].
- [14] J. Aichelin, P. B. Gossiaux and T. Gousset, Acta Phys. Polon. B **43** (2012) 655 [arXiv:1201.4192 [nucl-th]].